Antitumor Activity of the Novel Vascular Targeting Agent ZD6126 in a Panel of Tumor Models

David C. Blakey,[1] F. Russell Westwood, Mike Walker, Gareth D. Hughes, Peter D. Davis, Sue E. Ashton, and Anderson J. Ryan

Cancer and Infection Bioscience Department, AstraZeneca, Cheshire SK10 4TG [D. C. B., F. R. W., M. W., G. D. H., S. E. A., A. J. R.], and Angiogene Pharmaceuticals Ltd., Oxfordshire OX9 5SX [P. D. D.], United Kingdom

ABSTRACT

Purpose: **The purpose of this study was to examine the antitumor effects of the novel vascular targeting agent ZD6126 and to use histology, CD31 immunohistochemistry, and electron microscopy to gain an insight into the mechanism of action of this novel agent.**

Experimental Design: **The antitumor effects of ZD6126 were examined using a range of solid tumor models: (*a*) ras-transformed mouse 3T3 fibroblasts (Hras5); and (*b*) human lung (Calu-6), colorectal (LoVo and HT-29), prostate (PC-3), ovarian (SKOV-3), and breast (MDA-MB-231) tumors, grown as xenografts in nude mice.**

***Results: In vivo*, a well-tolerated dose of ZD6126 was shown to cause rapid effects on tumor endothelium leading to exposure of the basal lamina after cell retraction and subsequent loss of endothelial cells. This led to thrombosis and vessel occlusion, resulting in extensive tumor necrosis 24 h after ZD6126 administration. Dose-response studies showed that these effects were seen at a dose 8- to 16-fold lower than the maximum tolerated dose, demonstrating that ZD6126 has a wide therapeutic margin in these mouse models. A single dose of ZD6126 (200 mg/kg) led to a significant growth delay in Calu-6 and LoVo tumors. Growth delay was increased when 100 mg/kg ZD6126 was given as a well-tolerated regime in five daily doses. Finally, combining ZD6126 with cisplatin resulted in greater than additive enhancement in growth delay in the Calu-6 model.**

Conclusions: **These findings provide direct support that ZD6126 selectively disrupts tumor vasculature, demonstrate that it has activity in a range of tumor xenograft models, and show that it can significantly enhance the antitumor efficacy of cisplatin.**

INTRODUCTION

Solid tumors rely on a functioning vascular network for survival and growth, making tumor blood vessels a key target for potential therapeutic intervention. Tumor blood vessels differ significantly from vessels in normal tissues. For example, tumors contain a chaotic network of tortuous thin-walled vessels with a significant proportion of neovasculature because of a high proportion of proliferating endothelial cells (1). Specific features of tumor neovasculature that can be selectively targeted include adhesion molecule expression, altered coagulation control, and increased permeability (1). In addition, rapid endothelial cell proliferation may influence the differentiation characteristics of tumor vessels, resulting in immature endothelium and poorly formed vessels (1). As a therapeutic approach, vascular targeting aims to exploit the distinctive features of tumor vasculature to irreversibly arrest blood flow in tumors (2). The resulting ischemia leads to a rapid cascade of secondary tumor cell death and the destruction of central areas of a tumor normally resistant to conventional therapies (3–5). This vascular targeting strategy is therefore distinct from antiangiogenic approaches that aim to restrict tumor growth primarily by preventing new vessel formation (6).

One vascular targeting approach is to use antibodies or peptides that react with antigens selectively up-regulated on tumor endothelial cells to target agents that lead to tumor blood vessel occlusion (3, 7). An alternative strategy is to selectively disrupt rapidly proliferating and immature tumor endothelial cells based on their reliance on a tubulin cytoskeleton to maintain their cell shape. Antivascular activity is a common feature of tubulin-binding agents (4, 5, 8–10). Examples of such agents are colchicine, *Vinca* alkaloids, and combretastatins (11, 12). These agents exhibit both antimitotic and antivascular effects that lead to inhibition of spindle formation (mitotic arrest) and reduced tumor blood flow, respectively (10). Although tubulin-binding agents have antivascular activity, for most compounds the effects are only seen close to the MTD,[2] and direct tumor cell cytotoxicity via mitotic arrest appears to be the dominant mechanism of action (13, 14). However, combretastatin A-4 has demonstrated a selective effect against tumor vasculature at doses around one-third (12) to one-tenth (4) the MTD. Although the molecular mechanisms underlying the vascular effects are unknown, studies on combretastatins have shown that these tubulin-binding agents cause cytoskeletal disorganization (13), endothelial cell shape changes (5, 10, 12, 15–17), tumor vascular collapse (12), and reduced perfusion in tumors and some normal tissues (4, 18, 19).

ZD6126 is a novel vascular targeting agent that was devel-

Received 11/2/01; revised 3/14/02; accepted 3/15/02.
The costs of publication of this article were defrayed in part by the payment of page charges. This article must therefore be hereby marked *advertisement* in accordance with 18 U.S.C. Section 1734 solely to indicate this fact.

[1] To whom requests for reprints should be addressed, at Cancer and Infection Bioscience Department, AstraZeneca, Alderley Park, Macclesfield, Cheshire SK10 4TG, United Kingdom. Fax: 44-1625-513624; E-mail: david.blakey@astrazeneca.com.

[2] The abbreviations used are: MTD, maximum tolerated dose; NAC, *N*-acetylcolchinol; HPLC, high-performance liquid chromatography; EM, electron microscopy.

oped for its tubulin-binding properties and its ability to induce vascular damage in tumors. ZD6126 is a water-soluble prodrug of the tubulin-binding agent NAC. *In vitro*, at noncytotoxic doses, the drug disrupts the tubulin cytoskeleton, resulting in pronounced changes in cell morphology in proliferating endothelial cells but not in quiescent endothelial cells. *In vivo*, ZD6126 rapidly induces a large reduction in vascular volume and extensive necrosis in a murine tumor model, consistent with vascular rather than cytotoxic effects (20).

The aim of the current study was to examine the antitumor effects of ZD6126 and to gain a greater insight into the underlying mechanism of action of this novel agent. Specifically, we examined its spectrum of activity in a range of xenografted solid tumors and its histological effects on tumor endothelium. Because the drug was developed for vascular targeting and not direct tumor cell cytotoxicity, it has a distinct mechanism of action compared with standard chemotherapy. There is therefore interest in investigating the efficacy of ZD6126 in combination regimens with conventional anticancer agents. Because cisplatin is one of the most widely used chemotherapeutic drugs, we also studied tumor response to a combination of ZD6126 and cisplatin.

MATERIALS AND METHODS

Animals. Athymic nude mice (*nu/nu:Alpk*, 4–6 weeks of age) were used. Mice were given food and water *ad libitum*, and all animal procedures were carried out under a project license issued by the home office (London, United Kingdom) and performed according to United Kingdom Coordinating Committee on Cancer Research guidelines.

Compounds. ZD6126 was prepared as described elsewhere (20). Cisplatin was purchased as a 1 mg/ml solution from David Bull Laboratories (Warwick, United Kingdom). [^{14}C]ZD6126 was prepared from [methoxy-1-^{14}C]colchicine at a specific activity of 69.2 mCi/mg (30.2 mCi/mmol). [^{14}C]NAC, at a specific activity of 84.8 mCi/mg (30.3 mCi/mmol), was retained as an intermediate in the synthesis. The radiochemical purity, determined by thin-layer chromatography and HPLC, was >98% and >97%, respectively.

Plasma Clearance and Protein Binding. Plasma concentrations of ZD6126 and NAC were determined simultaneously by comparison with a calibration curve spiked with both compounds. The compounds were separated by HPLC [Phenomenex Prodigy 5-μm ODS3 analytical column (150 × 4.6-mm inside diameter)] using a CH_3CN:H_2O:HCOOH mobile phase and detected by tandem mass spectrometry (PE Sciex API 3000 spectrometer). The limits of quantification were 10 ng/ml for ZD6126 and NAC. Samples were collected at 10, 20, and 30 min and 1, 1.5, 2, 4, 6, 8, 12, and 24 h after ZD6126 dosing. Plasma protein binding was studied *in vitro* using plasma samples taken from 50 male and 50 female mice. Five 2-ml aliquots of plasma were spiked with 20 μl of [^{14}C]ZD6126 or [^{14}C]NAC solutions to give final concentrations of 0.01, 0.1, 1, 3, and 10 μg/ml and allowed to equilibrate in a shaking water bath for 10 min at 37°C. Duplicate 1-ml aliquots were then centrifuged at 1500 × *g* for 20 min, and the radioactive concentration of the ultrafiltrate was determined.

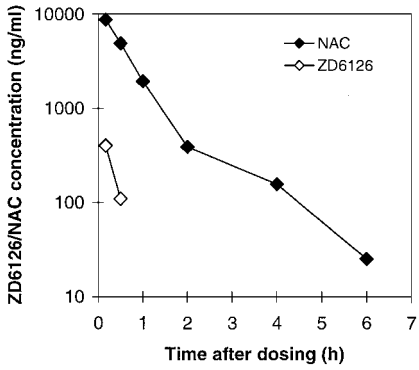

Fig. 1 Time *versus* plasma concentration profiles for ZD6126 and NAC after i.v. administration of 61 mg/kg ZD6126. Non-tumor-bearing nude mice were dosed with ZD6126, and plasma concentrations of ZD6126 and NAC were determined simultaneously by HPLC and tandem mass spectrometry. Two animals/time point were assessed at 11 time points (10 min to 24 h) after drug administration. After ZD6126 dosing, plasma ZD6126 and NAC were detectable only during the first 30 min and 6 h, respectively.

Cell Lines and s.c. Tumors. Calu-6 human lung cancer, HT-29 human colorectal cancer, LoVo human colorectal cancer, PC-3 human prostate cancer, SKOV-3 human ovarian cancer, and MDA-MB-231 human breast cancer cell lines were obtained from the American Type Culture Collection. The Hras5 cell line was isolated from mouse NIH 3T3 fibroblasts transfected with pT24C3 plasmid containing a mutant, transforming form of the *HRAS1* gene (ATCC 41000). Cell lines were maintained in DMEM (Hras5, Calu-6, LoVo, and MDA-MB-231), Ham's F-12 (SKOV-3), McCoy's 5A (HT-29), or Iscove's modified DMEM (PC-3), supplemented with 1% glutamine and 10% FCS in a humidified atmosphere of 95% air and 5% CO_2. Nude mice were implanted with Hras5 (2×10^5 or 2×10^6 cells), Calu-6 or HT-29 (10^6 cells in 50% Matrigel), or LoVo, SKOV-3, MDA-MB-231, or PC-3 (10^7 cells), and tumors were allowed to develop. Tumors were assessed by calipers using the formula $\pi/6 \times$ larger diameter × (smaller diameter)^2 to calculate tumor volume. Tumors were routinely grown to at least 0.20 cm^3 before drug treatment.

Tumor Necrosis. Necrosis was assessed by light microscopy. Tumor-bearing mice were treated with ZD6126 or PBS control, and tumors were excised 24 h later. After fixation in 10% buffered formalin and standard processing to paraffin wax blocks, sections (5 μm) were prepared and stained with H&E. The level of necrosis was scored subjectively by a pathologist using the following system: (*a*) grade 1, 0–10% necrosis; (*b*) grade 2, >10–20% necrosis; (*c*) grade 3, >20–30% necrosis; (*d*) grade 4, >30–40% necrosis; (*e*) grade 5, >40–50% necrosis; (*f*) grade 6, >50–60% necrosis; (*g*) grade 7, >60–70% necrosis; (*h*) grade 8, >70–80% necrosis; (*i*) grade 9, >80–90% necrosis; and (*j*) grade 10, >90–100% necrosis. The pathologist who graded the slides was blinded to the origin of the specimens to remove potential observer bias.

Histopathology, EM, and Immunohistochemistry. Nude mice bearing Hras5 s.c. tumors were sacrificed 30 min and 1, 2, and 4 h after dosing with 200 mg/kg ZD6126 i.p. or PBS vehicle control ($n = 2$ mice/group). For each tumor, a central

Table 1 Induction of tumor necrosis 24 h after administration of ZD6126 in a range of xenografted tumors

Tumors were grown to approximately 0.20–0.70 cm^3 and mice were treated with ZD6126 either i.v. (LoVo, Calu-6, and HT-29) or i.p. (Hras5, PC-3, SKOV-3, and MDA-MB-231). Twenty-four h later, tumors were excised, processed, and stained with H&E. The level of necrosis was scored with a 10-point grading system by a pathologist: grade 1, 0–10% necrosis; grade 2, >10–20% necrosis; grade 3, >20–30% necrosis; grade 4, >30–40% necrosis; grade 5, >40–50% necrosis; grade 6, >50–60% necrosis; grade 7, >60–70% necrosis; grade 8, >70–80% necrosis; grade 9, >80–90% necrosis; grade 10, >90–100% necrosis. Medians were calculated from $n > 6$ individual tumor measurements, except for HT-29 ($n = 4$). The significance of the difference between the median values of control and treated groups was assessed using the Mann-Whitney rank-sum test.

	Median necosis score[a]						
ZD6126 (mg/kg)	LoVo	Hras5	Calu-6	HT-29	PC-3	SKOV-3	MDA-MB-231
0	4 (3)	1 (0)	2 (1)	3.5 (1.5)	3 (1)	3 (1)	5 (1.25)
25	5 (1)	1 (2.75)	4.5[b] (2)	4 (0.5)	ND[c]	ND	ND
50	7[b] (2)	3.5[b] (2.5)	7[b] (2)	6.5[b] (2)	ND	ND	ND
100	8.5[b] (1.5)	6.5[b] (4)	8[b] (2)	8[b] (0.5)	ND	ND	ND
200	10[b] (2)	8[b] (2)	9[b] (1)	9.5[b] (1)	9[b] (1)	9[b] (1.25)	10[b] (0.25)

[a] Figures in parentheses are interquartile ranges calculated as the difference between the 75th and 25th percentiles.
[b] $P < 0.05$.
[c] ND, not done.

slice ~1–2-mm thick was fixed in 2.5% glutaraldehyde for subsequent processing to araldite blocks and preparation of toluidine blue-stained semi-thin (0.75 μm) sections. After assessing these sections, areas free from spontaneous necrosis were selected, and ultrathin (70–90 nm) sections prepared, stained with heavy metal salts, and examined on a Philips CM10 transmission electron microscope. Half of the remaining tumor tissue was fixed in 10% buffered formalin and embedded in paraffin wax, and H&E-stained sections were prepared. The other half was fixed for 12–48 h in zinc fixative (550523; BD PharMingen) before embedding in paraffin wax. Sections (3 μm) were then stained for CD31 using an avidin-biotin complex method. Endogenous peroxidase was blocked with 3% aqueous hydrogen peroxide, and proteins were blocked with a 1:20 dilution of normal rabbit serum (X0902; DAKO). Sections were then incubated at room temperature for 1 h with 100 μl of a 1:500 dilution of a rat monoclonal antimouse CD31 antibody (01951D; PharMingen). This was followed by the application of secondary [biotinylated rabbit antimouse (E0464; DAKO) or sheep antirabbit immunoglobulins (2AB02B; Serotec)] and tertiary (streptAB-complex/HRP; K0377; DAKO) antibodies with appropriate buffer washes. Visualization of antibody binding was performed by a diaminobenzidine chromogen procedure (HK153-5K; BioGenex).

Tumor Growth Delay. Athymic nude mice bearing established tumors were treated with PBS, ZD6126, cisplatin, or ZD6126 and cisplatin. The lengths and widths of tumors were measured three times a week using calipers, and volumes were calculated. Groups of 9–15 mice were included in each treatment group. Growth delay was determined by the difference in time taken for the mean tumor volume to double in treated *versus* control animals. Statistical comparisons were performed using a Mann-Whitney test.

RESULTS

Tolerability in Nude Mice. The maximum well-tolerated single dose of ZD6126 in athymic nude mice used in these studies was ~400 mg/kg, given either i.v. or i.p. This dose resulted in 8–18% body weight loss and no deaths ($n = 10$ mice; 5 males and 5 females) after i.v. dosing and 6% body weight loss and no deaths ($n = 2$ mice) after i.p. dosing. After a single dose of 200 mg/kg ZD6126 i.v., the only significant pathological finding was a mild reduction in cellularity of the bone marrow observed 24 h after drug administration ($n = 3$ mice). A similar mild to moderate effect on bone marrow was observed 24 h after treatment with five daily doses of 100 mg/kg ZD6126 i.v. ($n = 5$ mice).

Plasma Clearance and Protein Binding. Non-tumor-bearing nude mice were dosed with 61 mg/kg ZD6126, and plasma levels of ZD6126 and NAC were determined. ZD6126 was detected only at low levels after i.v. dosing and was undetectable in plasma 1 h after administration (Fig. 1). The highest concentration of NAC was observed at the earliest time point tested (8740 ng/ml at 10 min), indicating that ZD6126 is likely to be hydrolyzed rapidly to NAC, which is then cleared rapidly from the plasma (half-life, ~1 h). *In vitro* binding of [^{14}C]ZD6126 and [^{14}C]NAC to proteins in pooled plasma samples was independent of drug concentration and gender. Over the range of concentrations studied, the level of ZD6126 and NAC binding to plasma protein was 54 ± 1% (mean and SE of 10 values across all drug concentrations and genders) and 84 ± 1%, respectively.

Induction of Tumor Necrosis. Table 1 summarizes the dose-response data for induction of tumor necrosis after i.v. or i.p. administration of ZD6126 to mice bearing LoVo, Hras5, HT-29, or Calu-6 tumors. Significantly increased tumor necrosis was seen with 25–50 mg/kg ZD6126 in these tumor models. ZD6126 demonstrated a wide therapeutic margin (8- to 16-fold) in terms of its ability to cause a significant increase in tumor necrosis at doses well below the maximum well-tolerated dose studied (400 mg/kg). In studies comparing i.p. and i.v. administration of ZD6126 in the Hras5 model, the amount of necrosis was not significantly different by either route, indicating that in the mouse, the efficacy after dosing ZD6126 by either route is similar.[3] Table 1 also summarizes necrosis studies carried out in three additional tumor models (PC-3, SKOV-3, and MDA-MB-

[3] Unpublished data.

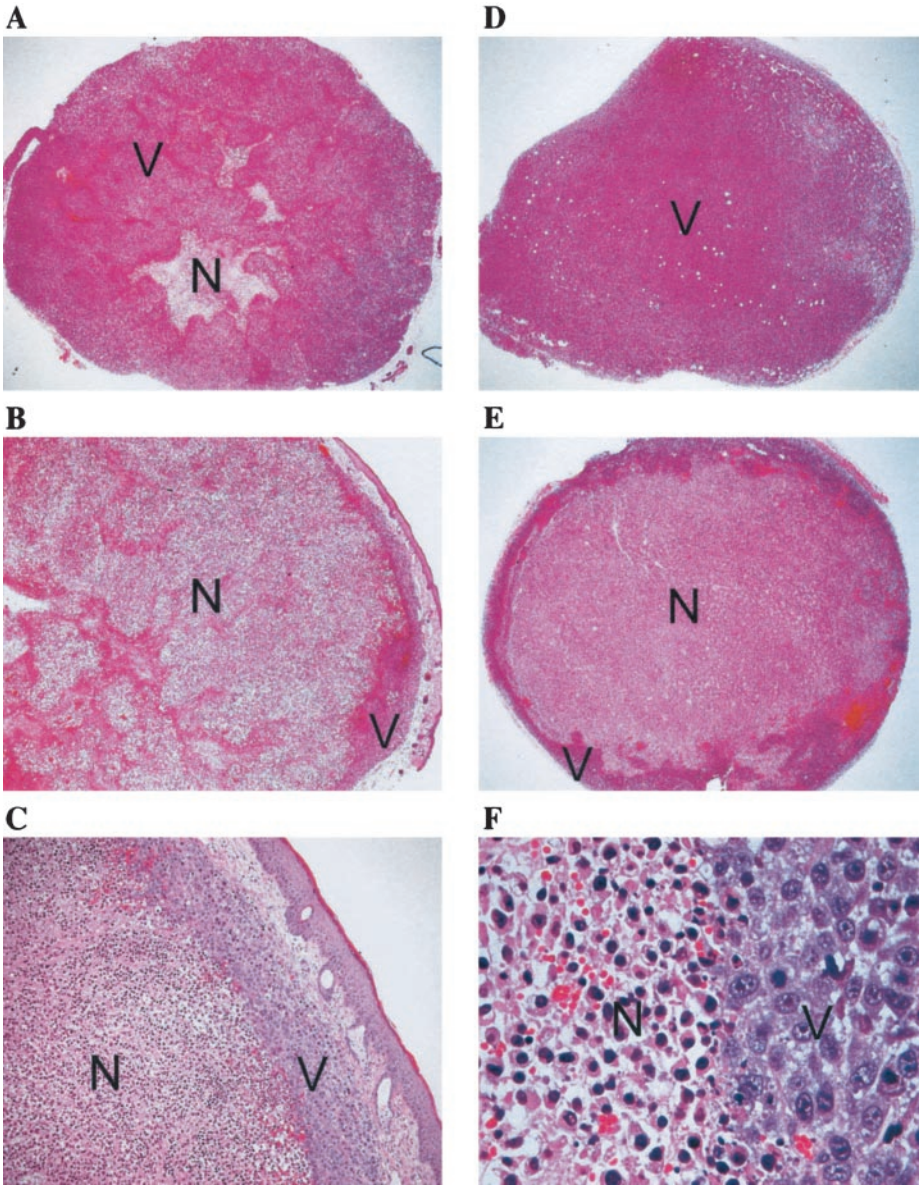

Fig. 2 ZD6126-induced tumor cell necrosis in the Calu-6 human lung cancer xenograft model and the Hras5 tumor model. Mice bearing Calu-6 (*A–C*) or Hras5 (*D–F*) tumors were treated with a single bolus dose of 200 mg/kg ZD6126 (*B*, *C*, *E*, and *F*) i.p. or vehicle control (*A* and *D*). Twenty-four h after treatment, tumors were excised and stained with H&E. Representative necrotic (*N*) and viable (*V*) regions of the tumors are identified. Vehicle-treated Calu-6 tumors (*A*) showed some areas of spontaneous central necrosis (median necrosis score, 2), whereas ZD6126-treated Calu-6 tumors (*B*) showed extensive central tumor necrosis (median necrosis score, 9) with only a thin rim of viable tumor cells (×16 magnification) that is more apparent at higher (×100) magnification (*C*). Vehicle-treated Hras5 tumors (*D*) showed little evidence of spontaneous necrosis (median necrosis score, 1), and ZD6126 treatment (*E*) induced extensive central tumor necrosis (median necrosis score, 8). At ×400 magnification (*F*), the contrast between viable Hras5 cells at the tumor rim and adjacent necrotic Hras5 cells toward the center of the tumor is evident.

231) where a single dose of 200 mg/kg ZD6126 resulted in extensive necrosis 24 h after drug administration. Fig. 2 illustrates these findings in Calu-6 and Hras5 tumors demonstrating a characteristic thin rim of viable tumor cells surrounding an extensive area of necrosis at the tumor core. A similar picture was observed in PC-3, HT-29, LoVo, SKOV-3, and MDA-MB-231 tumors.

Histopathology, EM, and Immunohistochemistry. Vehicle-treated Hras5 control tumors consistently showed only small areas of spontaneous necrosis that could be distinguished from ZD6126-induced necrosis by its different character and distribution; spontaneous necrosis was generally advanced and focal, whereas ZD6126-induced necrosis was seen as early and diffuse. Vessels within viable areas of the control tumors were generally not congested and showed an intact normal endothelium (Figs. 3*A*, 4*A*, and 5*A*) with endothelial cells lining the whole inner surface of the lumen (Fig. 5*A*). Thirty min after treatment with 200 mg/kg ZD6126 i.p., there were no changes in the light or electron microscope appearance of tumor cells and no changes in CD31 staining of endothelium. However, occasional thrombi were visible within tumor capillaries (Fig. 3*B*), and on ultrastructural assessment, there was focal loss of endothelial cell cytoplasm and exposure of basal lamina (Fig. 5*B*). These changes were associated with accumulation of platelets and fibrin. By 1 h, there was congestion of tumor vessels, and a number of thrombi were visible. Although CD31 staining appeared reduced in intensity, this may have been a result of attenuation of endothelial cells after vascular dilation. Two h after treatment, there was a slight pallor in H&E staining and an apparent shrinkage of tumor cells that affected all but the outer

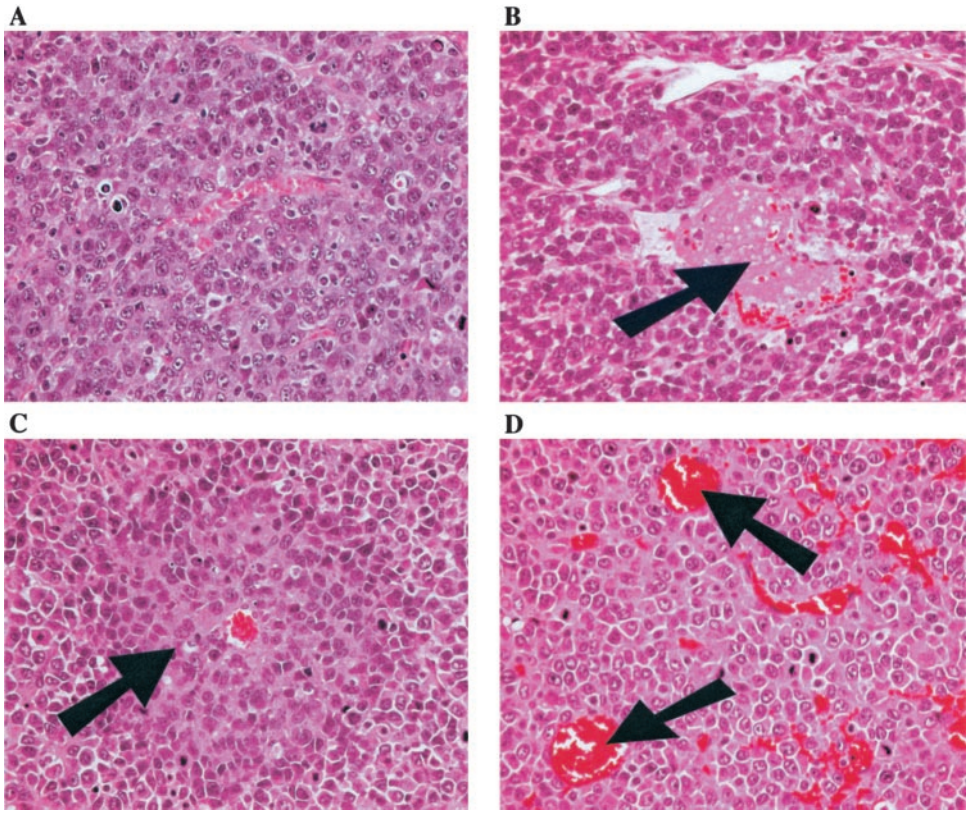

Fig. 3 ZD6126-induced blood vessel congestion and tumor cell necrosis in the Hras5 tumor model. Mice bearing Hras5 tumor xenografts were treated with a single bolus dose of 200 mg/kg ZD6126 i.p. or vehicle control. At various times after treatment, tumors were excised and stained with H&E and viewed at ×200 magnification. *A*, control sections showed normal capillaries with intact endothelium and viable tumor cells. *B*, 30 min after ZD6126 administration, thrombus formation within capillaries was evident (*arrow*). *C*, 4 h after administration of ZD6126, tumor cells distant from vessels had the shrunken, pale appearance of degenerate cells. Note the *halo* of spared tumor cells adjacent to a patent capillary (*arrow*). *D*, vascular congestion (*arrows*) with apparent loss of endothelial cells and diffuse tumor cell degeneration 4 h after administration of ZD6126.

rim of the tumor masses. This was supported by the ultrastructural appearance, which showed swelling and loss of subcellular organelles and the presence of ruptured cells and cellular debris. Many vessels were congested, showed areas of tunica intima with no positive CD31 staining (Fig. 4*B*), and, in terms of ultrastructure, showed frank loss of endothelium, packing of erythrocytes, and degranulated platelets and fibrin strands typical of thrombi (Fig. 5*C*).

Although tumor endothelial cells showed some evidence of subcellular degeneration, this was not as marked as in the surrounding tumor cells. At 4 h, changes were similar but more advanced than those at 2 h with pallor, shrinkage, and degeneration of tumor cells by H&E staining and ultrastructural assessment, sparing of the peripheral rim, and occasional sparing of tumor cells immediately adjacent to competent vessels (Fig. 3*C*). Generally, vessels were congested and showed occasional thrombi and loss of endothelial cells (Fig. 3*D*). These vessels were also devoid of CD31 staining (Fig. 4*C*). These effects of ZD6126 appeared selective for tumor endothelium because neither loss of CD31 staining (Fig. 4, *D and E*) nor vessel congestion[3] was apparent in the vasculature of surrounding nontumor tissue after drug treatment.

Time Course for Tumor Necrosis Induction. Fig. 6 illustrates a longer-term time course study for necrosis induction and subsequent regrowth in Calu-6 tumors after treatment with 200 mg/kg ZD6126 i.p. At early time points (1–4 h), the histological effects were consistent with the data reported above for Hras5 tumors (data not shown). After 24 h, increased tumor necrosis was seen with extensive central necrosis (>90–100% of tumor area), and a characteristic thin viable rim of tumor cells remained at the periphery. Histological analysis at 24, 48, 96, and 192 h demonstrated regrowth of the tumor from the residual rim of viable tumor cells (Fig. 6). A similar pattern of tumor regrowth was also seen in the more rapidly growing Hras5 tumor model. Four days after the 200 mg/kg ZD6126 i.p. treatment, the mean tumor necrosis score was 3.0, compared with a necrosis score of 10.0 at 24 h after treatment.

Tumor Growth Delay Studies. Table 2 illustrates the effect of single and multiple doses of ZD6126 on Hras5, Calu-6, and LoVo tumors. For Calu-6 tumors, a single dose of 200 mg/kg ZD6126 induced a 5.7-day growth delay, whereas in LoVo tumors, regressions associated with growth delays of 15.2, 12.8, and 9.4 days were obtained in three independent experiments. In a dose-response study carried out in LoVo tumors, significant antitumor effects were also seen at doses of 100 mg/kg (9.5-day growth delay) and 50 mg/kg (8.8-day growth delay), demonstrating that ZD6126 had significant antitumor activity in this model at a dose one-eighth of the maximum well-tolerated dose studied. A single dose of 200 mg/kg ZD6126 did not induce a significant growth delay in Hras5 tumors. Additional experiments examined the efficacy of multiple dose administration (100 mg/kg ZD6126 × 5 days; Table 2) in Calu-6 tumors, where two independent experiments produced growth delays of 10.1 and 10.7 days. In Hras5, the same multiple dose regime induced a small but significant tumor growth delay of 2.2 days.

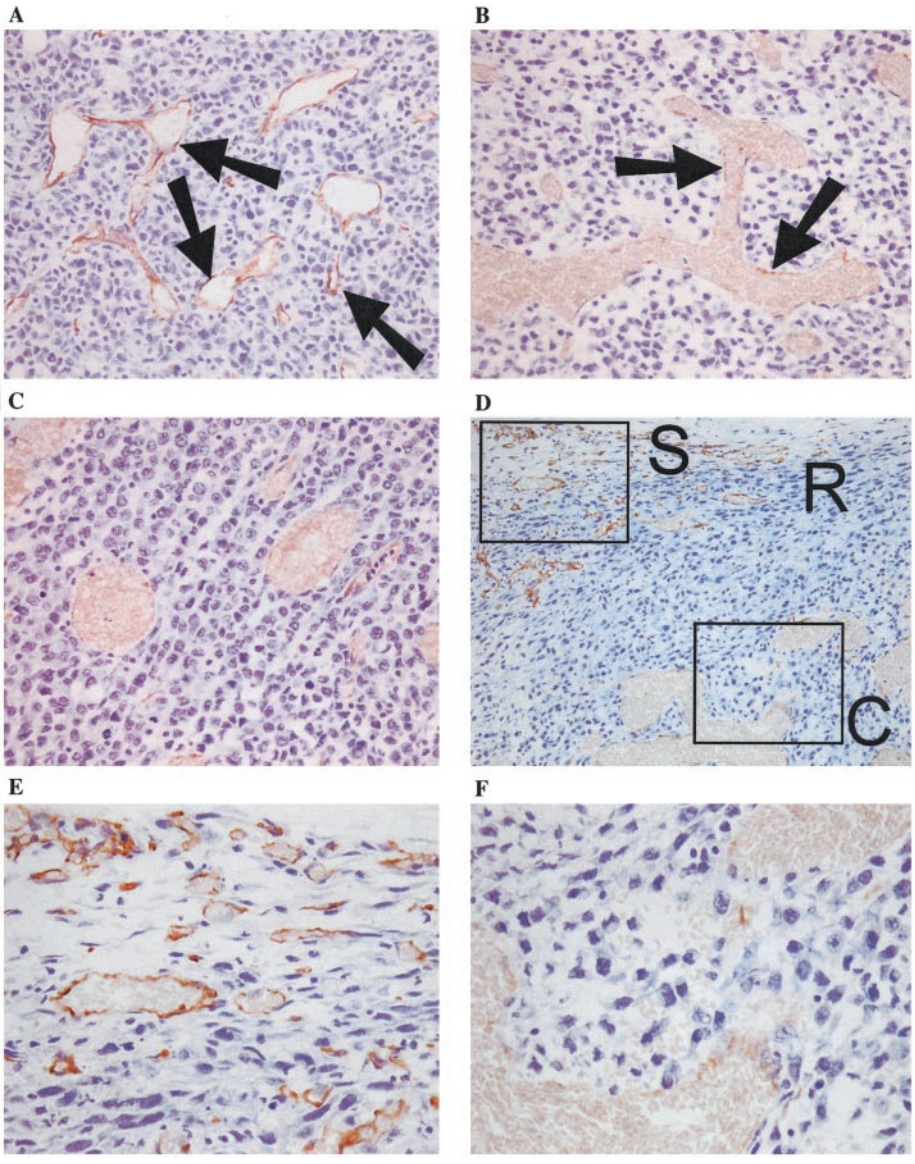

Fig. 4 CD31 immunohistochemistry. Mice bearing Hras5 tumor xenografts were treated with a single bolus dose of 200 mg/kg ZD6126 i.p. or vehicle control. At various times after treatment, tumors were excised and incubated with a rat antimouse CD31 primary antibody and, after staining, viewed at ×200 magnification. *A*, control tumors showed dark staining of intact endothelium (*arrows*). *B*, patchy staining of residual endothelial cells was apparent 2 h after ZD6126 treatment (*arrows*). *C*, 4 h after ZD6126 treatment, there was almost total absence of staining of endothelial cells. *D*, 4 h after ZD6126 treatment, viewed at ×100 magnification, the rim (*R*) of the tumor and the surrounding normal connective tissue (*S*) showed dark staining of intact endothelium. In contrast, there was little staining of endothelial cells in the core of the tumor (*C*). The areas identified by the *upper* and *lower boxes* are shown at ×400 magnification in *E* and *F*, respectively, and demonstrate that the effects of ZD6126 treatment on loss of CD31 staining are selective for tumor vasculature, in particular, vasculature at the tumor core.

Combination of ZD6126 with Cisplatin. In two independent experiments, 4 mg/kg cisplatin i.p. and ZD6126 (100 mg/kg × 5 days) i.p. produced modest growth delays in Calu-6 xenografts growing in nude mice (6.0 and 3.9 days for cisplatin; 10.1 and 10.7 days for ZD6126). Administration of 4 mg/kg cisplatin i.p. 24 h before ZD6126 (100 mg/kg × 5 days) i.p. resulted in Calu-6 tumor regression and prolonged growth delays of 20.5 and 19.7 days in each of the two experiments. Fig. 7 shows the tumor growth curves for one experiment only. The growth delay seen was greater than the sum of the growth delays for ZD6126 and cisplatin given as single agents in two independent experiments.

DISCUSSION

ZD6126 was well tolerated in mice in both single and multiple dose regimens. Doses of ZD6126 that produced pronounced vascular targeting activity were associated with minimal toxicity in nude mice. Pharmacokinetic studies showed that ZD6126 was rapidly metabolized to NAC and that NAC was rapidly cleared from plasma. Similar studies in rats and dogs have demonstrated that glucuronide is the major metabolite of NAC and that it is eliminated predominantly through the fecal route, whereas little or no ZD6126 is excreted unchanged into urine or feces.[3] The moderate level of protein binding (probably to serum albumin) in human plasma suggests that this compound is unlikely to be involved in clinically significant protein binding displacement interactions.

Although antivascular activity is a common feature of tubulin-binding agents, for most compounds the effects are only seen at or close to the MTD, and direct tumor cell cytotoxicity is the predominant mechanism of action. ZD6126 was developed to have vascular targeting activity by optimizing its tubulin

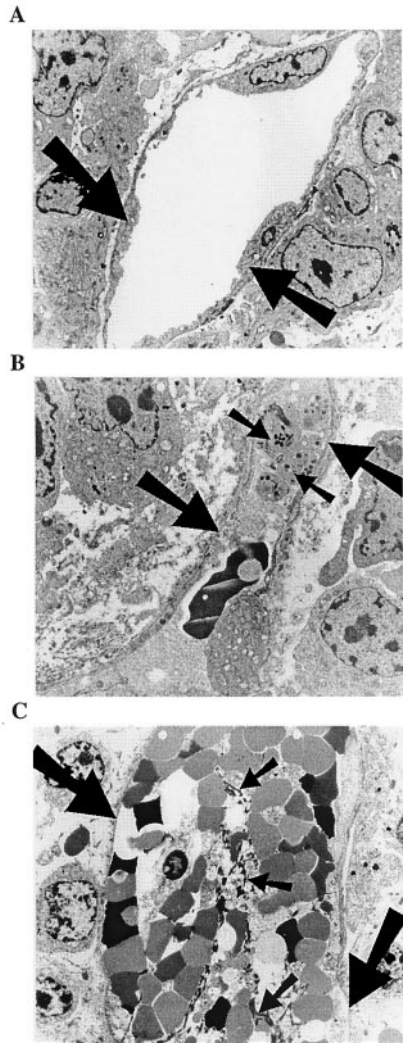

Fig. 5 Ultrastructural images of ZD6126-treated Hras5 tumors. Mice bearing Hras5 tumor xenografts were treated with a single bolus dose of 200 mg/kg ZD6126 i.p. or vehicle control. At various times after treatment, tumors were excised, and sections were prepared for EM. *A*, ×2750 magnification. Control tumors showed intact normal endothelium (*large arrows*). *B*, ×3800 magnification. Thirty min after ZD6126 attenuated endothelium, multifocal exposure of basement membranes (*large arrows*) and accumulation of platelets (*small arrows*) with deposition of fibrin were apparent. *C*, ×1900 magnification. Two h after ZD6126, there was extensive loss of endothelial cells (*large arrows*) with thrombosis; note the degranulated platelets and fibrin deposition (*small arrows*).

binding and pharmacokinetic properties while minimizing cytotoxicity (20). Our dose-response studies of necrosis induction showed that the effects of ZD6126 were seen at a dose one-eighth to one-sixteenth the maximum well-tolerated dose studied. This is consistent with a previous report using a mouse breast tumor model (CaNT), where significant antitumor activity was seen at a dose one-thirtieth the MTD of ZD6126 in CBA mice (20). Combretastatin derivatives have demonstrated vascular targeting activity at doses around one-third (12) to one-tenth (4) of the MTD, although direct comparison with ZD6126 in the same tumor model has not been reported.

An important finding of this study is the direct visualization by EM of effects on endothelial cells by ZD6126 within 30 min of administration to mice bearing Hras5 tumors. Loss of endothelial cell cytoplasm leading to exposure of the basal lamina is consistent with the rapid morphological effects (contraction of the tubulin cytoskeleton and rounding up of endothelial cells) reported in proliferating endothelial cells *in vitro* (20). At later time points, both EM and CD31 staining indicated a loss of tumor endothelial cells that is consistent with the endothelial cell detachment seen *in vitro* after ZD6126 treatment of proliferating endothelial cells (21). At these early time points, there was no evidence of direct cytotoxic effects on the tumor cells surrounding tumor blood vessels. In addition, there was no evidence at any time point of morphological effects on endothelial cells in normal vessels, confirming the selectivity of ZD6126 for the tumor vasculature.

The effects seen on the tumor vascular endothelium resulted in the rapid congestion of tumor blood vessels. Although evidence of activated platelets and deposition of fibrin was seen by EM, it is not clear whether clotting was a secondary event or played a major role in this process. The use of agents that interfere with the clotting process might be useful to determine the role of clotting in tumor vascular occlusion. After ZD6126-induced vascular occlusion, a cascade of tumor cell death was seen, with tumor cells distant from the blood vessels dying at earlier time points than those adjacent to the blood vessel in both the Hras5 model and Calu-6 model. This pattern of cell death is consistent with death because of nutrient starvation rather than direct cytotoxicity and provides further support for a vascular damage-mediated mechanism of action of ZD6126 rather than a direct tumor cytotoxic effect. Within 24 h of administration of ZD6126 (100–200 mg/kg), the entire center of the tumor in all of the models examined was necrotic, with a thin viable rim of tumor cells surviving at the periphery in all cases. This pattern of central necrosis and a thin viable rim of tumor cells is also seen in vascular targeting approaches using antibodies to selectively target toxins or coagulating proteins to the tumor (3, 22) and with combretastatin A-4 and is again consistent with ZD6126 acting as a vascular targeting agent. Taxol or cisplatin administration at doses that cause growth delays in Calu-6 tumors results in no significant increase in necrosis at 24 h,[3] confirming that these effects on the tumor seen with ZD6126 are unlikely to be attributable to a low level of cytotoxic activity. It is thought that the viable rim of tumor cells survives because it receives nutrients and removes waste products via adjacent normal blood vessels that are unaffected by selective tumor vascular targeting agents. However, direct evidence for this hypothesis is not available. The consequence of this viable rim is that after cessation of treatment, the central necrotic portion of the tumor is replaced with a viable tumor that grows back from this rim. In the Hras5 tumor model, this regrowth was very rapid and probably explains why a single dose of 200 mg/kg ZD6126 i.p. in this model did not result in a significant tumor growth delay despite causing massive central necrosis 24 h after drug treatment. In the Calu-6 model, where regrowth from the peripheral rim of the tumor was slower, a single dose of ZD6126 induced a significant tumor growth delay. The clinical potential of ZD6126 in human disease, where solid tumors would be

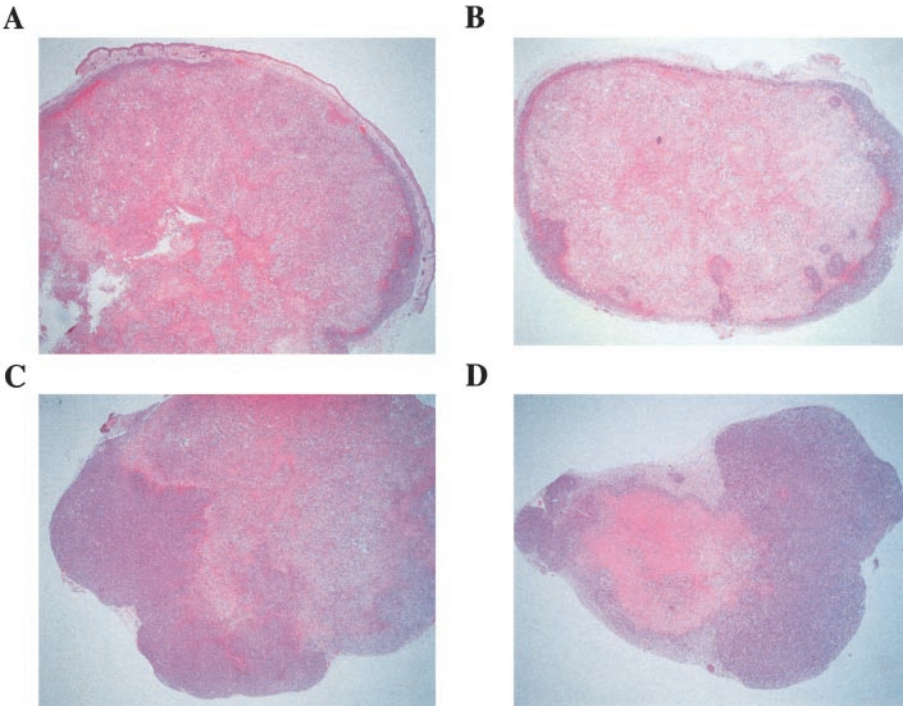

Fig. 6 Regrowth of Calu-6 tumors after a single dose of ZD6126. Mice bearing Calu-6 tumor xenografts were treated with a single bolus dose of 200 mg/kg ZD6126 i.p. At various times after ZD6126 treatment, tumors were excised, stained with H&E, and viewed at ×16 magnification. *A*, 24 h; median necrosis score, 10. *B*, 48 h; median necrosis score, 9. *C*, 96 h; median necrosis score, 7. *D*, 192 h; median necrosis score, 7. Regrowth appears to originate from the tumor rim.

Table 2 ZD6126-induced tumor growth delays

Tumor	ZD6126 dose (mg/kg) and schedule[a]	Growth delay (days)[b]
Hras5	200 × 1	0.5 (NS)
Hras5	100 × 5	2.2
LoVo	50 × 1	8.8
LoVo	100 × 1	9.5
LoVo	200 × 1	15.2, 12.8, and 9.4
Calu-6	200 × 1	5.7
Calu-6	100 × 5	10.1 and 10.7

[a] ZD6126 was administered as a single bolus dose of 50–200 mg/kg or as bolus doses of 100 mg/kg on 5 consecutive days (total dose, 500 mg/kg). Growth delay was determined by the difference in time taken for tumors to double in volume in ZD6126-treated animals compared with saline-treated controls.

[b] Growth delays were significant ($P < 0.05$), except where stated. NS, not significant.

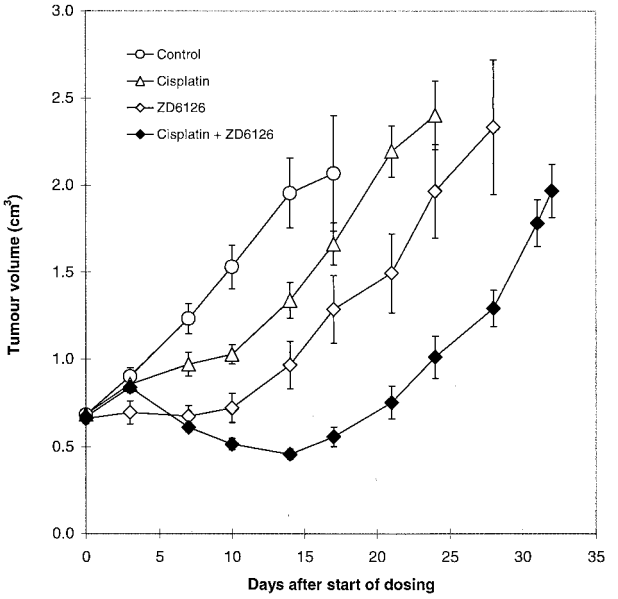

Fig. 7 Growth of Calu-6 human tumor xenografts after treatment with 4 mg/kg cisplatin i.p. and ZD6126 i.p. (100 mg/kg × 5 days) alone and in combination. The lengths and widths of tumors were measured three times a week using calipers, and mean tumor volumes were calculated for each group. Groups of 9–15 mice were included in each treatment group.

expected to grow much more slowly, may be affected by the rate of repopulation of the necrotic tumor core.

One way to address tumor regrowth is to give multiple doses of ZD6126. In these studies, giving five daily doses of ZD6126 (100 mg/kg) resulted in increased growth delays in both the Hras5 and Calu-6 tumors. Presumably, the subsequent doses of ZD6126 prevented regrowth by destroying the neovasculature induced to support the growing rim, although direct experimental data to support this hypothesis were not generated. Similar increases in growth delay with ZD6126 were seen in multiple daily dosing studies in a syngeneic breast mouse tumor model (20). In a future clinical setting, the dose schedule of ZD6126 required to achieve maximal antitumor activity may reflect the likely differences in tumor repopulation rates between mouse and human tumors.

An alternative strategy to address cell survival in the peripheral tumor rim is to combine ZD6126 with cytotoxic drugs or radiation. Because the edge of the tumor xenograft is likely to be well perfused from surrounding vessels in normal tissues, this

tumor compartment may provide a good target for such standard agents. It was shown previously that both antivascular and antiangiogenic agents could enhance the effects of standard chemotherapeutic drugs (23, 24). Therefore, to address this issue, we studied the efficacy of ZD6126 combined with cisplatin, a widely used cytotoxic drug. A greater than additive growth delay was seen in the Calu-6 lung tumor model. Similar interactions have been reported using combretastatin derivatives combined with cisplatin (25), 5-fluorouracil (26), doxorubicin (27), and radiation (28). It is not known what mechanism lies behind the greater than additive interaction seen when combining ZD6126 and cisplatin. However, ZD6126 appears most effective at killing the central region of the tumor that is likely to be hypoxic and have reduced cellular proliferation. Therefore, ZD6126 may be ideally suited to complement the action of radiation and cytotoxic drugs that would be expected to have greatest activity against the well-oxygenated proliferating component of tumors. Although the timing of drug administration may be important (in these studies, we gave the cisplatin 24 h before ZD6126), a similar growth delay was seen when cisplatin was given either 24 h before or 24 h after combretastatin A-4 phosphate (25). Additional data on scheduling cytotoxic drugs and radiation with vascular targeting agents will be important to help optimize their clinical utility.

These studies have demonstrated that ZD6126 has activity across a spectrum of human xenograft tumors (colorectal, prostate, breast, ovarian, and lung), consistent with an effect on the tumor vasculature rather than the tumor cell compartment. Classical cytotoxic and antihormonal agents tend to have greater activity against specific tumor types, whereas a vascular targeting agent might be expected to have utility across many solid tumors. Tumors in these studies varied in weight from approximately a 0.20–0.70-g equivalent to approximately 0.5–1.75-kg tumors in a 60-kg person. Over this size range, a single dose of ZD6126 induced around 90% necrosis 24 h after drug administration in all of the tumors studied. The effect of a combretastatin derivative, AC-7700, has been shown to be similar toward small and large tumors (29), confirming the views from this work that tubulin-binding agents are effective vascular targeting drugs over a range of tumor sizes. In animal models, combretastatins have shown potential to be effective against xenografts, orthotopic tumors, and tumor metastases, although there is evidence that combretastatins may be more effective against larger tumors and are inactive against avascular metastatic deposits (12). Potentially, vascular targeting agents will be effective toward any cancer that relies on neovasculature, whether it is a small disseminated metastasis or a large primary tumor (1, 30).

In conclusion, well-tolerated doses of ZD6126 are active against many tumor xenografts growing in mice. The early effects on endothelial cells and the time course and pattern of tumor necrosis are consistent with vascular targeting activity. Significant growth delay was induced when ZD6126 was given as a single agent, and effects were increased using either multiple daily doses or ZD6126 in combination with cisplatin. These studies confirm that ZD6126 is a novel vascular targeting agent with promising activity in experimental solid tumor models. On the basis of these encouraging findings, Phase I studies are now in progress to examine the potential of ZD6126 in the treatment of human cancer.

ACKNOWLEDGMENTS

We thank Rebecca Somers, Simon Brocklehurst, and Zena Wilson for technical support.

REFERENCES

1. Denekamp, J. Vascular attack as a therapeutic strategy for cancer. Cancer Metastasis Rev., *9:* 267–282, 1990.

2. Chaplin, D. J., and Dougherty, G. J. Tumor vasculature as a target for cancer therapy. Br. J. Cancer, *80* (Suppl. 1)*:* 57–64, 1999.

3. Huang, X. M., Molema, G., King, S., Watkins, L., Edgington, T. S., and Thorpe, P. E. Tumor infarction in mice by antibody-directed targeting of tissue factor to tumor vasculature. Science (Wash. DC), *275:* 547–550, 1997.

4. Dark, G. G., Hill, S. A., Prise, V. E., Tozer, G. M., Pettit, G. R., and Chaplin, D. J. Combretastatin A-4, an agent that displays potent and selective toxicity toward tumor vasculature. Cancer Res., *57:* 1829–1834, 1997.

5. Otani, M., Natsume, T., Watanabe, J. I., Kobayashi, M., Murakoshi, M., Mikami, T., and Nakayama, T. TZT-1027, an antimicrotubule agent, attacks tumor vasculature and induces tumor cell death. Jpn. J. Cancer Res., *91:* 837–844, 2000.

6. Randal, J. Antiangiogenesis drugs target specific cancers, mechanisms. J. Natl. Cancer Inst. (Bethesda), *92:* 520–522, 2000.

7. Nilsson, F., Kosmehl, H., Zardi, L., and Neri, D. Targeted delivery of tissue factor to the ED-B domain of fibronectin, a marker of angiogenesis, mediates the infarction of solid tumors in mice. Cancer Res., *61:* 711–716, 2001.

8. Baguley, B. C., Holdaway, K. H., Thomsen, L. L., Shuang, L., and Zwi, L. I. Inhibition of growth of colon 38 adenocarcinoma by vinblastine and colchicine. Evidence for a vascular mechanism. Eur. J. Cancer, *27:* 482–487, 1991.

9. Hill, S. A., Lonergan, S. J., Denekamp, J., and Chaplin, D. J. Vinca alkaloids: antivascular effects in a murine tumor. Eur. J. Cancer, *29A:* 1320–1324, 1993.

10. Nihei, Y., Suzuki, M., Okano, A., Tsuji, T., Akiyama, Y., Takashi, T., Saito, S., Hori, K., and Sato, Y. Evaluation of antivascular and antimitotic effects of tubulin binding agents in solid tumor therapy. Jpn. J. Cancer Res., *90:* 1387–1396, 1999.

11. Woods, J. A., Hadfield, J. A., Pettit, G. R., Fox, B. W., and McGown, A. T. The interaction with tubulin of a series of stilbenes based on combretastatin A-4. Br. J. Cancer, *71:* 705–711, 1995.

12. Grosios, K., Holwell, S. E., McGown, A. T., Pettit, G. R., and Bibby, M. C. *In vivo* and *in vitro* evaluation of combretastatin A-4 and its sodium phosphate prodrug. Br. J. Cancer, *81:* 1318–1327, 1999.

13. Rowinsky, E. K., Cazenave, L. A., and Donehower, R. C. Taxol: a novel investigational antimicrotubule agent. J. Natl. Cancer Inst. (Bethesda), *82:* 1247–1259, 1990.

14. Hill, S. A., Sampson, L. E., and Chaplin, D. J. Antivascular approaches to solid tumor therapy: evaluation of vinblastine and flavone acetic acid. Int. J. Cancer, *63:* 119–123, 1995.

15. Watts, M. E., Woodcock, M., Arnold, S., and Chaplin, D. J. Effects of novel and conventional anticancer agents on human endothelial permeability: influence of tumor-secreted factors. Anticancer Res., *17:* 71–75, 1997.

16. Tozer, G. M., Prise, V. E., Wilson, J., Locke, R. J., Vojnovic, B., Stratford, M. R., Dennis, M. F., and Chaplin, D. J. Combretastatin A-4 phosphate as a tumor vascular-targeting agent: early effects in tumors and normal tissues. Cancer Res., *59:* 1626–1634, 1999.

17. Galbraith, S. M., Chaplin, D. J., Lee, F., Stratford, M. R. L., Locke, R. J., Vojnovic, B., and Tozer, G. M. Effects of combretastatin A-4 phosphate on endothelial cell morphology *in vitro* and relationship to tumour vascular targeting activity *in vivo*. Anticancer Res., *21:* 93–102, 2001.

18. Beauregard, D. A., Thelwall, P. E., Chaplin, D. J., Hill, S. A., Adams, G. E., and Brindle, K. M. Magnetic resonance imaging and spectroscopy of combretastatin A4 prodrug-induced disruption of tumor perfusion and energetic status. Br. J. Cancer, *77:* 1761–1767, 1998.

19. Hori, K., Saito, S., Nihei, Y., Suzuki, M., and Sato, Y. Antitumor effects due to irreversible stoppage of tumor tissue blood flow: evaluation of a novel combretastatin A-4 derivative, AC7700. Jpn. J. Cancer Res., *90:* 1026–1038, 1999.

20. Davis, P. D., Hill, S. A., Galbraith, S. M., Chaplin, D. J., Naylor, M. A., Nolan. J., and Dougherty, G. J. ZD6126: a new agent causing selective damage of tumor vasculature. Proc. Am. Assoc. Cancer Res., *41:* 329, 2000.

21. Blakey, D. C., Douglas, S., Revill, M., and Ashton, S. A. The novel vascular targeting agent ZD6126 causes rapid morphology changes leading to endothelial cell detachment at noncytotoxic concentrations. Clin. Exp. Metastasis, *17:* 776, 1999.

22. Thorpe, P. E., and Derbyshire, E. J. Targeting the vasculature of solid tumors. J. Control. Release, *48:* 277–288, 1997.

23. Teicher, B. A., Sotomayor, E. A., and Huang, Z. D. Antiangiogenic agents potentiate cytotoxic cancer therapies against primary and metastatic disease. Cancer Res., *52:* 6702–6704, 1992.

24. Pruijn, F. B., van Daalen, M., Holford, N. H., and Wilson, W. R. Mechanisms of enhancement of the antitumor activity of melphalan by the tumor-blood-flow inhibitor 5,6-dimethylxanthenone-4-acetic acid. Cancer Chemother. Pharmacol., *39:* 541–546, 1997.

25. Chaplin, D. J., Pettit, G. R., and Hill, S. A. Antivascular approaches to solid tumor therapy: evaluation of combretastatin A4 phosphate. Anticancer Res., *19:* 189–195, 1999.

26. Grosios, K., Loadman, P. M., Swaine, D. J., Pettit, G. R., and Bibby, M. C. Combination chemotherapy with combretastatin A-4 phosphate and 5-fluorouracil in an experimental murine colon adenocarcinoma. Anticancer Res., *20:* 229–233, 2000.

27. Nelkin, B. D., and Ball, D. W. Combretastatin A-4 and doxorubicin combination treatment is effective in a preclinical model of human medullary thyroid carcinoma. Oncol. Rep., *8:* 157–160, 2001.

28. Li, L. Y., Rojiani, A., and Siemann, D. W. Targeting the tumor vasculature with combretastatin A-4 disodium phosphate: effects on radiation therapy. Int. J. Radiat. Oncol. Biol. Phys., *42:* 899–903, 1998.

29. Nihei, Y., Suga, Y., Morinaga, Y., Ohishi, K., Okano, A., Ohsumi, K., Hatanaka, T., Nakagawa, R., Tsuji, T., Akiyama, Y., Saito, S., Hori, K., Sato, Y., and Tsuruo, T. A novel combretastatin A-4 derivative, AC-7700, shows marked antitumor activity against advanced solid tumors and orthotopically transplanted tumors. Jpn. J. Cancer Res., *90:* 1016–1025, 1999.

30. Denekamp, J. Angiogenesis, neovascular proliferation, and vascular pathophysiology as targets for cancer therapy. Br. J. Radiol., *66:* 181–186, 1993.

Clinical Cancer Research

Antitumor Activity of the Novel Vascular Targeting Agent ZD6126 in a Panel of Tumor Models

David C. Blakey, F. Russell Westwood, Mike Walker, et al.

Clin Cancer Res 2002;8:1974-1983.